Studies on the effect of blend ratio and crosslinking system on thermal, X-ray and dynamic mechanical properties of blends of natural rubber and ethylene–vinyl acetate copolymer

Alex T. Koshy, Baby Kuriakose*†, Sabu Thomas and S. Varghese†
School of Chemical Sciences, Mahatma Gandhi University, Kottayam 686631, Kerala, India
(Received 30 April 1992; revised 19 October 1992)

Differential scanning calorimetry (d.s.c.), X-ray, dynamic mechanical and microscopy studies were carried out using a series of blends of natural rubber (NR) and ethylene–vinyl acetate copolymer (EVA) in the crosslinked and uncrosslinked states. The crosslinking system (sulfur, peroxide and mixed) and blend ratio do not influence significantly the melting temperature (T_m) of EVA. The decrease in percentage crystallinity of EVA with NR content is related to the incomplete crystallization, as indicated by the lower heat of fusion (ΔH). The glass transition temperature (T_g) of NR in the uncrosslinked blend did not change substantially and this indicated incompatibility. However, in the case of crosslinked systems, depending on the type of crosslinking agents used, the T_g of the NR phase in the blend was shifted to higher temperatures. This has been explained with reference to the predominant crosslinking of the NR phase. From X-ray diffraction patterns, the interplanar distances (d values) were calculated. With the addition of NR there was a tendency for the d values to increase in all systems. The crystallinity was measured by X-ray and the results were in line with those of d.s.c. measurements. The dynamic mechanical properties such as tan δ, storage modulus and loss modulus of the blends were evaluated. The existence of separate T_g values in dynamic mechanical thermal analyser studies indicates that the blends are incompatible. The morphology of the uncrosslinked blends has been studied by scanning electron microscopy.

(Keywords: blends; d.s.c.; crosslinking systems; X-ray analysis; d.m.t.a.; natural rubber; ethylene–vinyl acetate copolymer)

INTRODUCTION

The concept of appropriately combining two or more different polymers to obtain a new material system with the desirable features of its constituents is not new. Over he years, numerous systems based on the chemical ombination of different monomers through random, block and graft copolymerization methods have been developed with this goal in mind. For similar reasons, the coatings and rubber industries have blended together different polymers and particularly over the last decade the interest in polymer blend systems as a way to meet new market applications with minimum development cost has rapidly increased. This approach has not been without its difficulties and has not developed as rapidly as it might, in part because most physical blends of different high-molecular-weight polymers prove to be immiscible. That is, when mixed together, the blend components are likely to separate into phases containing predominantly their own kind. This characteristic, combined with the often low physical attraction forces across the phase boundaries, usually causes immiscible blend systems to have poor mechanical properties. Even for immiscible pairs, proper control of phase morphology during processing and addition of compatibilizing agents can improve the interfacial situation.

In recent years the technical literature on this subject has expanded greatly, as evidenced by the appearance of several research papers, books and proceedings of various conferences[1–6]. Martuscelli *et al.*[7,8] have reported on the thermal behaviour and morphology of rubber–plastic blends. According to them, fundamental information about the miscibility of blends and the phase diagram of the components in the molten state could be obtained from these studies. Locke and Paul[9] studied the dynamic mechanical properties, thermal behaviour, adhesion characteristics and morphology of ternary blends to examine the effectiveness of a third component as a blend modifier. Kuriakose and De[10] and Thomas *et al.*[11] have also investigated morphology, miscibility and mechanical properties of various thermoplastic elastomer blends.

Recently, blends of natural rubber (NR) and ethylene–vinyl acetate copolymer (EVA) have gained a lot of interest. These materials combine the excellent ageing and flex crack resistance of EVA and the good mechanical properties of NR. In this laboratory, we have already studied the mechanical properties, vulcanization kinetics, rheological behaviour and ageing properties of these blends[12–16]. The present study explores the miscibility, morphology, crystallization and dynamic

*To whom correspondence should be addressed
†Present address: Rubber Research Institute of India, Kottayam 686009, Kerala, India

0032-3861/93/163428-09

mechanical properties of NR–EVA blends with special reference to the effects of blend ratio and crosslinking systems.

EXPERIMENTAL

Materials

Natural rubber (NR) conforming to ISNR 5 was supplied by the Rubber Research Institute of India.

Ethylene–vinyl acetate (EVA Exxon 218) was supplied by the Exxon Chemical Company, Houston. The vinyl acetate content of EVA is 18% by weight, its melt flow index is 1.7 g per 10 min and the Vicat softening point is 64°C. All other additives such as dicumyl peroxide (DCP), zinc oxide (ZnO), sulfur, and dibenzthiazyl disulfide (MBTS) were of commercial grade.

Blend preparation

The blends were prepared in a laboratory model intermix (Shaw Intermix KO) set at a temperature of 80°C and a rotor speed of 60 r.p.m. NR was masticated for 2 min and then blended with EVA for 2.5 min. The final temperature of the blend inside the intermix was in the range 110–125°C, depending upon the blend ratio.

The blends contained 0, 30, 40, 50, 60, 70 and 100% by weight of EVA and were designated A, D, E, F, G, H and J, respectively. The blends were compounded in a two-roll laboratory mill as per the test recipes given in *Table 1*. The compounds which contained the sulfur cure system were designated A_1, D_1 and F_1 and those with DCP as A_2, D_2, F_2, H_2 and J_2. Compounds which contained the mixed cure system consisting of sulfur and DCP were designated as A_3, D_3, F_3, H_3 and J_3. The proportions of sulfur and DCP in the mixed cure system did not correspond to the proportions of NR and EVA in the blend because their distribution in these two elastomers can be different[12]. As given in *Table 1*, the mixed cure system contained the sum of the curatives used for the sulfur and DCP systems. The objective of taking these three cure systems was to study the responses of polysulfidic, carbon–carbon and mixed crosslinks towards thermal and dynamic mechanical effects. The compounded blends were vulcanized to optimum cure in a steam-heated hydraulic press at 160°C to get the required test samples. The blends with 50% or more of EVA could not be vulcanized fully with the sulfur system and hence could not be evaluated for physical properties.

The blends were characterized by differential scanning calorimetry (d.s.c.), X-ray, scanning electron microscopy (SEM) and dynamic mechanical thermal analysis (d.m.t.a.).

Table 1 Formulations of mixes in g per 100 g of rubber

Ingredients	Sulfur system	DCP system	Mixed system
Polymer	100.0	100.0	100.0
Zinc oxide	5.0	5.0	5.0
Stearic acid	1.5	1.5	1.5
Styrenated phenol antioxidant	1.0	1.0	1.0
Dibenzthiazyl disulfide	0.8	–	0.8
Dicumyl peroxide (40% active ingredient)	–	4.0	4.0
Sulfur	2.5	–	2.5

Differential scanning calorimetry

The thermal behaviour of the blends was studied with the help of a Perkin–Elmer DSC-4 thermal analyser. The samples were inserted into the apparatus at room temperature and immediately heated to 200°C at a rate of 40°C min^{-1} and kept for 1 min at this temperature in order to remove the volatile impurities. The samples were quenched to −110°C at the rate of 320°C min^{-1}. The d.s.c. scan was made from −110 to 120°C at the rate of 20°C min^{-1}. The glass transition temperature of each sample was taken as the midpoint of the step in the scan. The peak maximum from the d.s.c. curve was considered as the melting point.

X-ray study

In order to find out the degree of crystallinity and the amorphous content of different blends, X-ray diffraction patterns of the samples were recorded with an X-ray diffractometer using Ni-filtered CuKα radiation from a Philips X-ray generator. The angular range was 5 to 40° (2θ). Samples of the same thickness and the same area were exposed. The operating voltage and the current of the tube were kept at 55 kV and 190 mA, respectively, throughout the course of the investigation.

The X-ray diffraction patterns of the samples were separated into two parts, crystalline and amorphous, by taking natural rubber as fully amorphous. The areas under the crystalline and amorphous portions were measured in arbitrary units, and the degree of crystallinity X_c and the amorphous content X_a of the samples were calculated using the relations

$$X_c = \frac{I_c}{I_c + I_a}$$

$$X_a = \frac{I_a}{I_a + I_c}$$

where I_c and I_a represent the integrated intensities corresponding to the crystalline and amorphous phases, respectively, i.e. the areas under the respective curves.

Dynamic mechanical thermal analysis

Dynamic mechanical measurements were carried out on a dynamic mechanical thermal analyser (Polymer Laboratories) consisting of a temperature programmer and controller. This instrument measures dynamic moduli (both storage and loss moduli) and the damping of a specimen under an oscillatory load as a function of temperature. The experiment was conducted in uniaxial tension mode from −80 to +20°C at a frequency of 10 Hz at 0.325% dynamic strain with a programmed heating rate of 1°C min^{-1}. Liquid nitrogen was used to achieve subambient temperatures. The mechanical loss factor $\tan\delta$ and the dynamic moduli E' and E'' were calculated with a microcomputer.

Scanning electron microscopy

The SEM observations of the blends were made using a JEOL 35C scanning electron microscope. One end of the uncrosslinked blend in cylindrical form was kept immersed in benzene for about 48 h to extract the NR phase. These samples were then dried at 40°C in an air oven without disturbing the extracted surface and their surfaces were examined under the SEM for the morphology study. Photographs of the extracted surface were taken at 1000× magnification in all cases.

Table 2 Thermal properties of NR–EVA blends

Properties	Uncrosslinked blend					Crosslinked blend[a]							
	A	D	F	H	J	D_1	F_1	D_2	F_2	H_2	D_3	F_3	H_3
Heat of fusion ΔH (cal g^{-1})	–	1.8	3.7	4.8	5.2	1.9	3.6	1.9	4.6	3.9	1.9	4.7	4.3
Peak temperature T_m (°C)	–	85.3	84.9	83.9	86.7	85.3	85.0	81.0	81.5	79.4	81.4	81.6	82.0
Onset of glass transition (°C)	−67.4	−71.2	−70.3	−70.2	−35.7	−69.1	−67.9	−65.7	−65.4	−65.0	−64.4	−65.5	−66.0
Glass transition temperature T_g (°C) } NR phase	−65.3	−66.3	−66.9	−66.5	–	−58.0	−54.6	−63.8	−62.7	−63.0	−57.1	−53.4	−43.8
Glass transition temperature T_g (°C) } EVA phase	–	–	–	–	−27.0	–	–	–	–	–	–	–	–
Crystallinity (%)	–	11.2	23.3	29.0	32.1	11.6	22.2	11.5	28.4	24.1	11.7	29.0	26.6

[a]The subscripts 1, 2 and 3 stand for sulfur, peroxide and mixed cure systems, respectively

RESULTS AND DISCUSSION

Thermal properties

The thermal properties of NR, EVA, and crosslinked and uncrosslinked blends were analysed by d.s.c. The melting temperatures T_m, fractional crystallinities X_c, heats of fusion ΔH and glass transition temperatures T_g of the blends are reported in *Table 2*.

D.s.c. results for the uncrosslinked and crosslinked blends are given in *Figures 1* and *2*, respectively. The peak point temperature of the thermogram was taken as the melting point T_m. It is interesting to note from *Table 2* that in the case of uncrosslinked and sulfur-crosslinked blends, T_m is almost independent of composition. However, a slight decrease in melting point is observed in the case of peroxide-cured and mix-cured blends.

The area of the melting endotherm is also calculated and reported as the heat of fusion ΔH. The fractional crystallinities of EVA in the blends are calculated from the ΔH values on the basis that EVA has an 18% vinyl acetate content[17]. It is seen that the fractional crystallinity X_c and heat of fusion values decrease with increase in rubber content for similar conditions of crystallization. The crystallinity of EVA was found to be 32%. With gradual incorporation of NR, the crystallinity of EVA comes down to 29.0% for 30:70 NR:EVA, 13.3% for 50:50 NR:EVA and 11.6% for 70:30 NR:EVA blends. Martuscelli[8] has shown that crystallinity is affected by blend composition and crystallization conditions such as temperature, pressure, orientation, molecular weight and diluent. The crystallization of the EVA segments is controlled by the segmental diffusion rate of the other polymeric chains. The separation is enhanced as the NR content is increased. Incomplete crystallization thus leads to a decrease in ΔH and, hence, crystallinity.

The glass transition temperatures T_g as obtained from the d.s.c. measurements are reported in *Table 2* for crosslinked and uncrosslinked NR–EVA blends. The T_g values of pure NR and EVA are found to be −65.3°C and −27.0°C, respectively. In the case of uncrosslinked NR–EVA blends, the glass transition temperature of NR was found to be −66°C. It is interesting to note that the T_g value of the NR phase remains almost constant with increasing composition. The T_g of the EVA phase could not be detected in the blends using d.s.c. However, d.m.t.a. (see later) could detect the T_g of EVA. It seems that the T_g values of the two phases in the uncrosslinked blends do not undergo substantial shifts. These observations, coupled with the fact that T_m remains more or less constant with increase in NR content, indicate the fact that the blends are incompatible or immiscible[18].

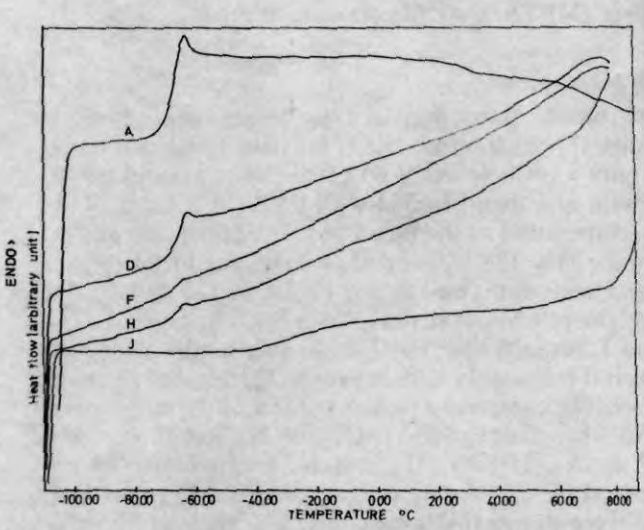

Figure 1 D.s.c. thermograms of uncrosslinked NR–EVA blends

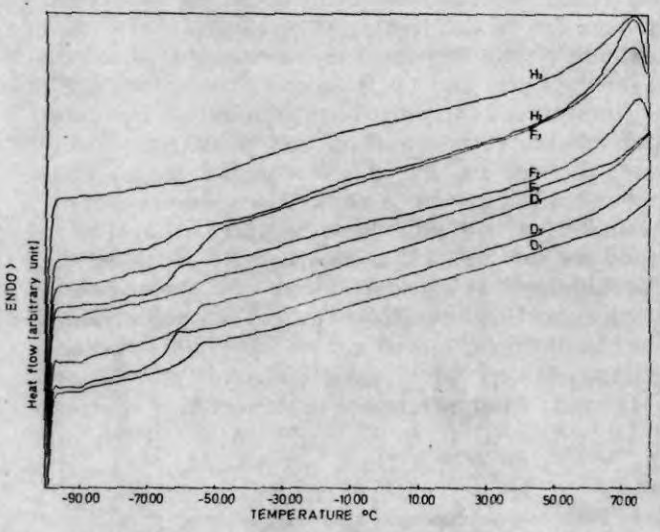

Figure 2 D.s.c. thermograms of crosslinked NR–EVA blends

It is interesting to note that in the case of crosslinked blends, depending on the type of crosslinking system used (sulfur, peroxide or mixed) the T_g of the NR phase undergoes a substantial shift from its normal position to a higher temperature (*Table 2*). Generally, the introduction of crosslinks increases the T_g value due to the restriction of the segmental motion of the polymer by the crosslinks. When sulfur is used as the crosslinking

system, the NR phase is preferentially crosslinked. DCP crosslinks both the phases. In the mixed system, sulfur crosslinks the NR phase and DCP crosslinks both the phases. In the case of the 70:30 NR:EVA blend, the T_g values of the NR phase in the blend for the sulfur, peroxide and mixed crosslink systems are −58.0, −63.8 and −57.1°C, respectively. The T_g of the natural rubber phase in the uncrosslinked 70:30 NR:EVA blend is −66.3°C. This suggests that the increase in the T_g of the NR phase is at its maximum when the mixed system is used as the crosslinking agent. A similar behaviour was observed for 50:50 and 30:70 NR:EVA blends. Therefore, it can be concluded that the mixed system predominantly crosslinks the NR phase and the crosslinking efficiency of the three systems in the NR phase varies in the order mixed > sulfur > peroxide. Since

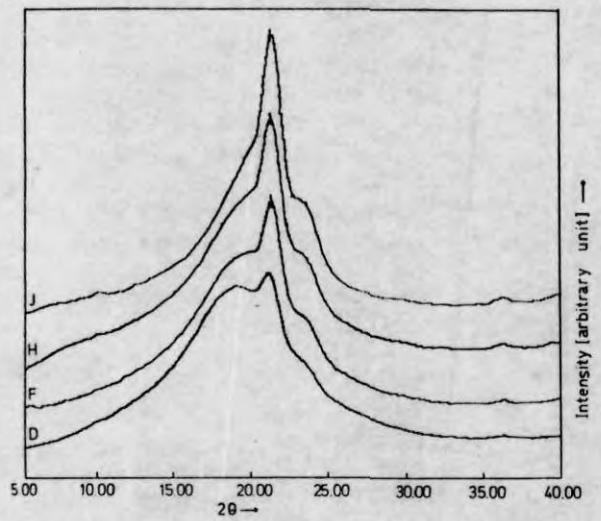

Figure 3 X-ray diffraction patterns of uncrosslinked NR–EVA blends

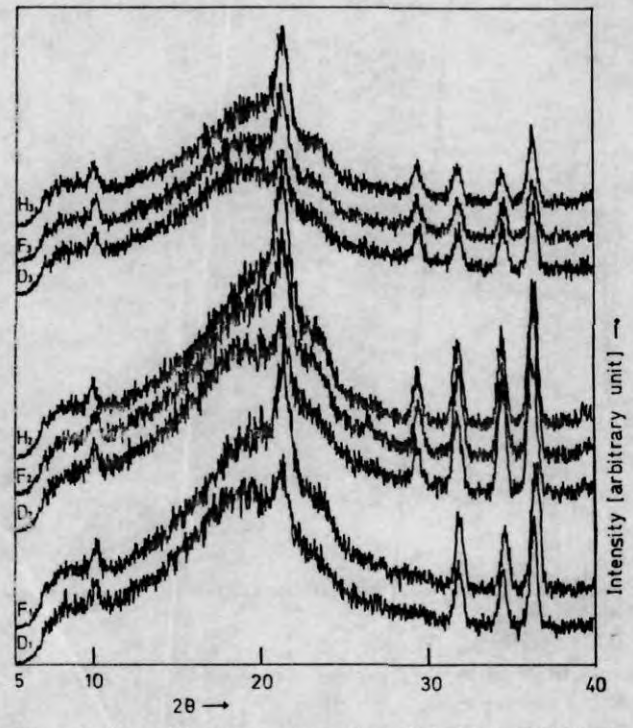

Figure 4 X-ray diffraction patterns of crosslinked NR–EVA blends

Table 3 Crystallization characteristics of the blends

Sample reference	Crystallinity X_c (%)	d values (Å)
Uncrosslinked		
Sample D	10.3	4.164 3.799 2.499
Sample F	24.6	4.164 3.796 2.493
Sample H	26.5	4.164 3.786 2.483
Sample J	36.4	4.164 3.776 2.473
Crosslinked[a]		
Sample D_1	7.6	4.165 3.800 2.494
Sample F_1	20.1	4.164 3.797 2.493
Sample D_2	7.6	4.164 3.799 2.495
Sample F_2	20.4	4.165 3.798 2.493
Sample H_2	22.6	4.165 3.777 2.473
Sample D_3	7.7	4.166 3.800 2.495
Sample F_3	20.4	4.164 3.799 2.495
Sample H_3	22.1	4.165 3.776 2.473

[a]The subscripts 1, 2 and 3 stand for sulfur, peroxide and mixed cure systems

the resolution of the equipment used for the study was only up to 15 nm, the T_g corresponding to the EVA phase could not be detected and therefore the extent of crosslinking in the EVA phase could not be derived.

X-ray diffraction analysis

Figures 3 and *4* depict the X-ray diffraction patterns of uncrosslinked and crosslinked blends. The results of the X-ray analyses of the samples are given in *Table 3*. From the table it can be seen that the degree of crystallinity X_c of EVA is 36.4%. This is higher than that obtained by d.s.c. measurements. The value of X_c depends very much on the method of preparation of the sample and the technique of measurement[19]. The decrease in crystallinity caused by natural rubber is due to the addition of an amorphous component which migrates into the crystalline phase of pure EVA, reducing the crystalline domains of the pure EVA sample. The introduction of crosslinks further reduces the crystallinity of the system. This is due to the fact that the crosslinking system arrests the regular arrangement of the crystalline

regions within the sample[14]. The interplanar distances (d values) are reported in *Table 3*. With the addition of natural rubber there was a tendency for the d value to increase in most systems. This suggests the migration of the NR phase into the interchain spaces of EVA. Similar observations have been reported in the case of NR–PE blends by Roychoudhury *et al.*[18].

Microscopy studies

Figure 5a is the photomicrograph of blend G, the composition of which is 60:40 EVA:NR. The holes seen on the surface are formed by the extraction of the NR phase. At this blend ratio NR remains as dispersed particles in the EVA matrix. The sizes of the dispersed particles are also small compared with their sizes in those blends which contain a higher proportion of NR. As the proportion of NR in the blend is increased to 50% (blend F), the sizes of the holes have increased several-fold (*Figure 5b*). The boundary of EVA that separates the holes has narrowed down to a thin layer. When the EVA:NR ratio is 40:60 (blend E), this narrow boundary layer is broken since it is unable to withstand the forces due to the swelling of the NR phase (*Figure 5c*). It is possible that in blends E and F both NR and EVA form continuous phases because of the higher proportion of the NR phase and the lower melt viscosity of the EVA phase[14]. The photomicrograph of the 30:70 EVA:NR blend shows aggregates of EVA domains lying on the benzene-extracted surface (*Figure 5d*), indicating that phase inversion has occurred in the blend and EVA forms the dispersed phase at this blend ratio. Thus, the morphology of uncrosslinked EVA NR blends appears to be such that the EVA forms the dispersed phase when its proportion is below 40% and NR forms the dispersed phase when its proportion is 40% or below. In the range of 40:60 and 50:50 EVA:NR both the polymers remain as continuous phases to give an interpenetrating structure.

Dynamic mechanical properties

The dynamic mechanical behaviours of crosslinked and uncrosslinked systems are shown in *Figures 6* to *17*. The glass transition temperature was selected at the peak position of tan δ and E'' when plotted as a function of temperature. The T_g values of all the systems are given in *Table 4*.

The tan δ values of uncrosslinked blends as a function of temperature are given in *Figure 6*. It is seen that pure NR exhibits a transition at $-46^{\circ}C$. For pure EVA the transition is detected at $-10^{\circ}C$. All the blends exhibit

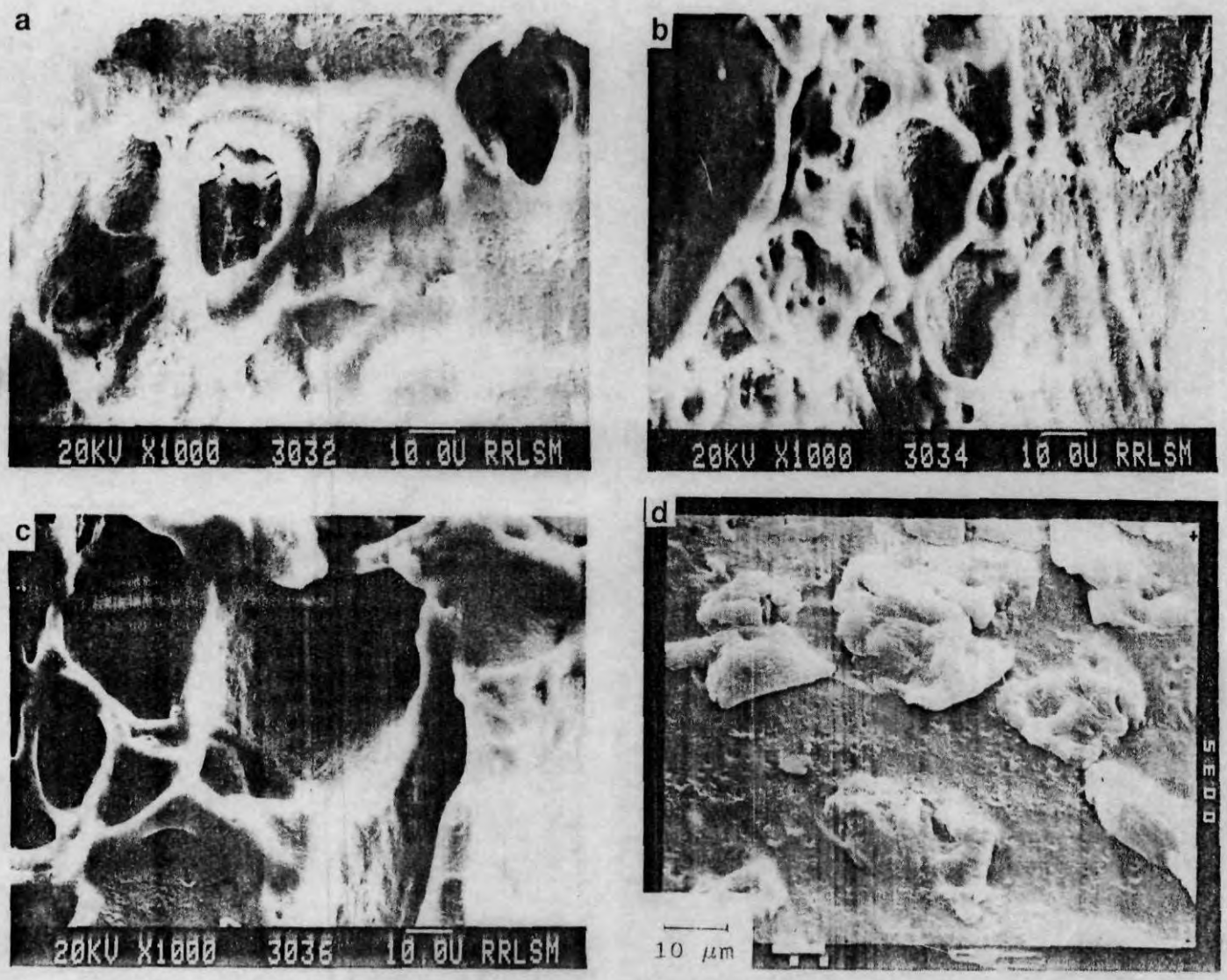

Figure 5 (a) Photomicrograph of blend G. (b) Photomicrograph of blend F. (c) Photomicrograph of blend E. (c) Photomicrograph of blend D

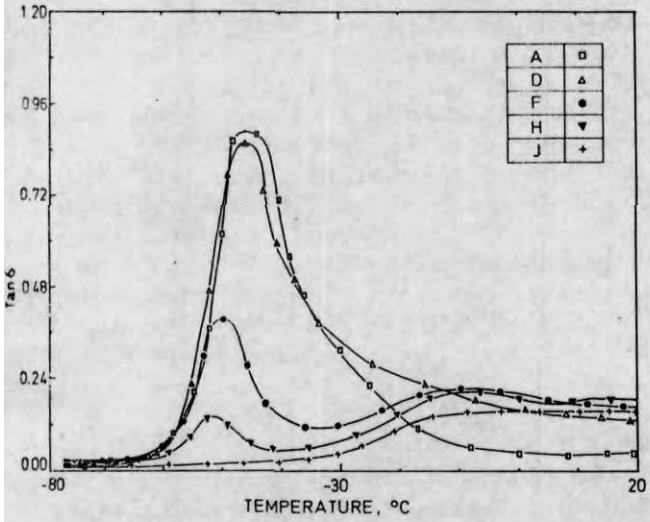

Figure 6 Effect of temperature on the loss tangent of uncrosslinked NR–EVA blends

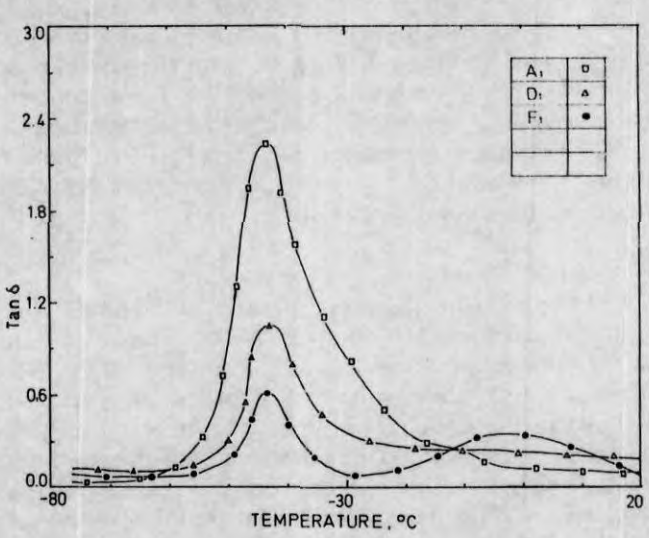

Figure 9 Effect of temperature on the loss tangent of sulfur-cured NR–EVA blends

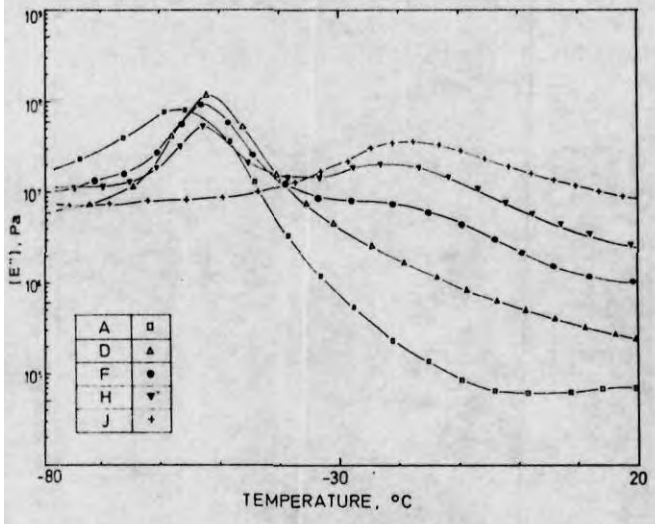

Figure 7 Effect of temperature on the loss modulus of uncrosslinked NR–EVA blends

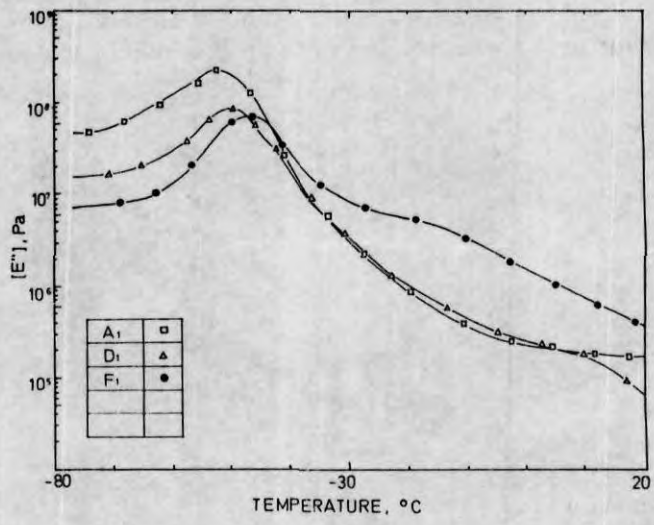

Figure 10 Effect of temperature on the loss modulus of sulfur-cured NR–EVA blends

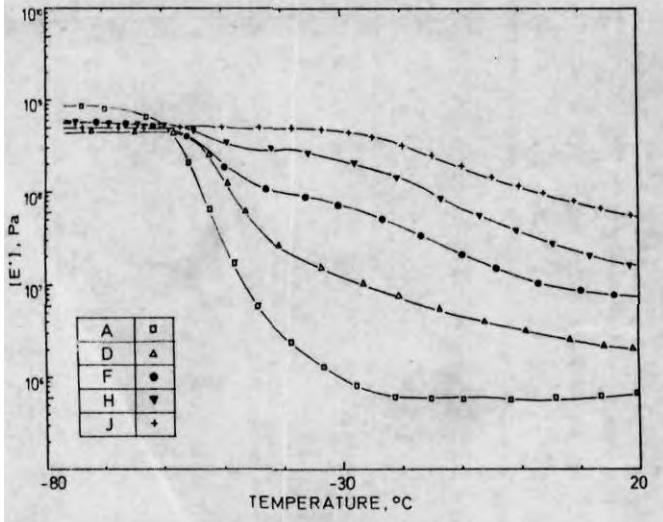

Figure 8 Effect of temperature on the storage modulus of uncrosslinked NR–EVA blends

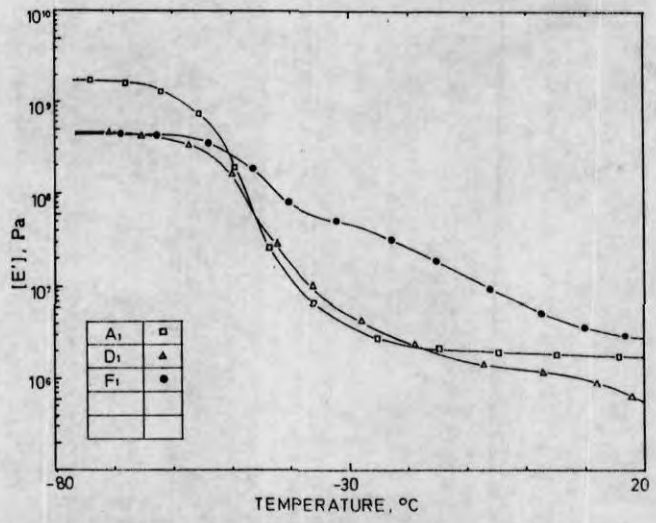

Figure 11 Effect of temperature on the storage modulus of sulfur-cured NR–EVA blends

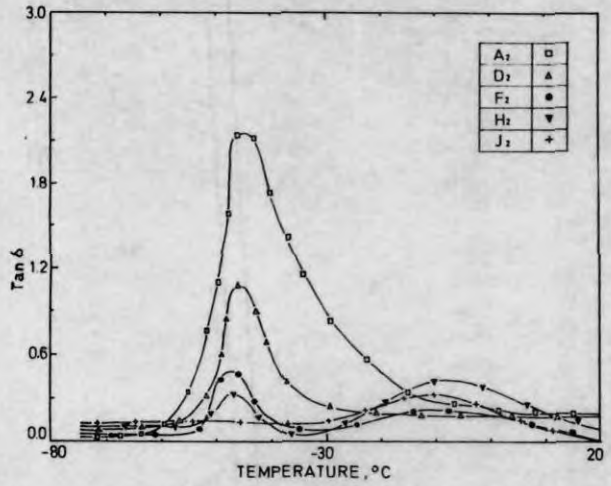

Figure 12 Effect of temperature on the loss tangent of peroxide-cured NR–EVA blends

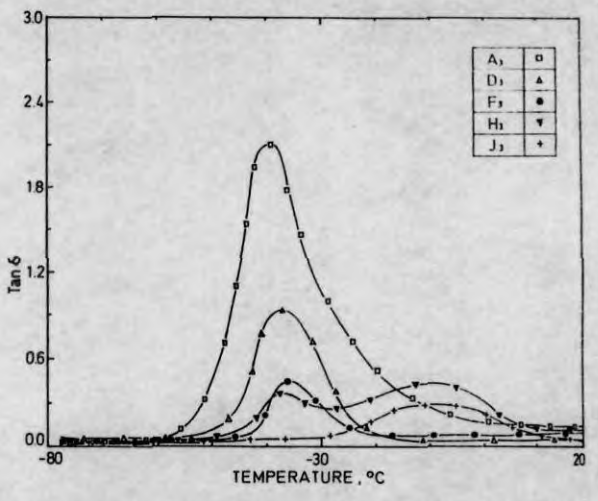

Figure 15 Effect of temperature on the loss tangent of mix-cured NR–EVA blends

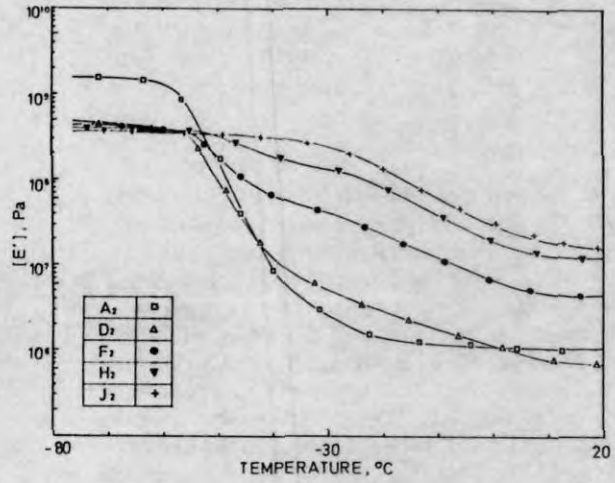

Figure 13 Effect of temperature on the storage modulus of peroxide-cured NR–EVA blends

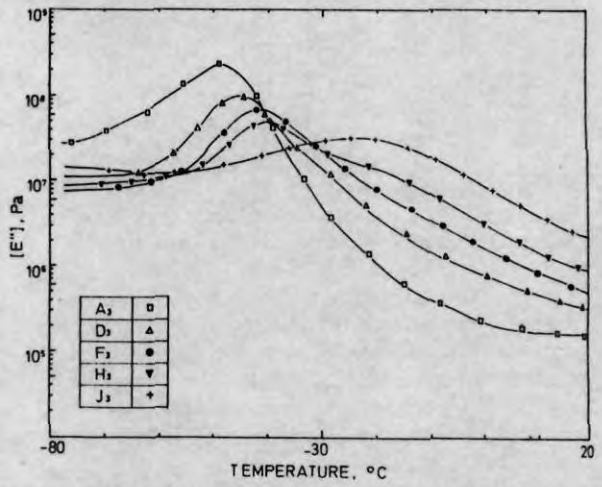

Figure 16 Effect of temperature on the loss modulus of mix-cured NR–EVA blends

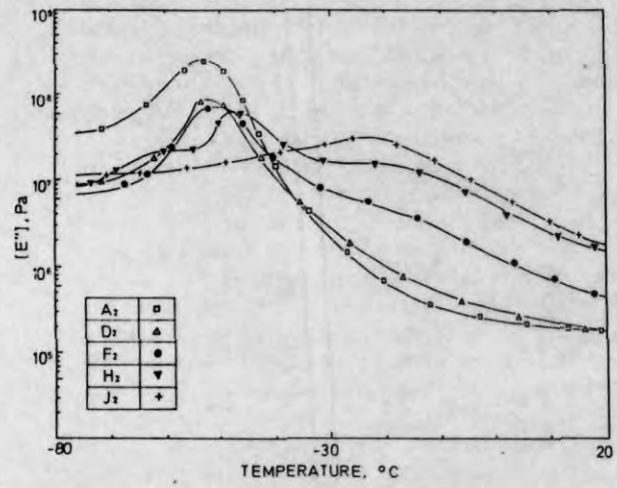

Figure 14 Effect of temperature on the loss modulus of peroxide-cured NR–EVA blends

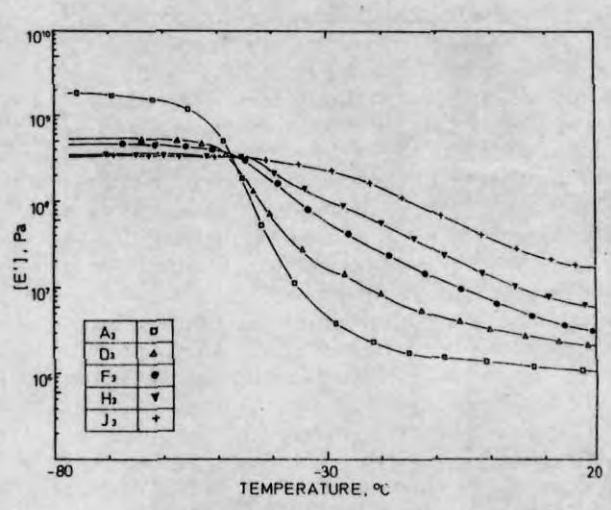

Figure 17 Effect of temperature on the storage modulus of mix-cured NR–EVA blends

Table 4 Dynamic mechanical properties

Sample reference	T_g, NR phase (°C)	T_g, EVA phase (°C)	tan δ_{1max} NR phase	E (kJ mol^{-1})	tan δ_{2max} EVA phase	E'' peak temperature of NR transition (°C)	E'' peak temperature of EVA transition (°C)
Sample A (0:100)	−46.3	–	–	211.12	–	−55.0	–
Sample D (70:30)	−46.3	–	0.856	205.50	–	−51.0	–
Sample F (50:50)	−50.0	−10.9	0.400	178.45	0.200	−51.0	−20.4
Sample H (30:70)	−51.7	−10.1	0.165	191.29	0.200	−51.0	−20.4
Sample J (100:0)	–	−10.0	–	–	0.144	–	−20.0
Sample A_1	−42.0	–	2.200	204.62	–	−51.1	–
Sample D_1	−42.3	–	1.020	170.89	–	−48.0	–
Sample F_1	−43.6	−5.0	0.880	161.46	0.280	−45.0	−20.0
Sample A_2	−45.0	–	2.200	209.84	–	−53.1	–
Sample D_2	−46.0	–	1.040	218.23	–	−52.6	–
Sample F_2	−48.0	−10.0	0.440	176.05	0.224	−50.0	−20.0
Sample H_2	−47.5	−8.0	0.224	216.35	0.400	−46.3	−20.0
Sample J_2	–	−10.0	–	–	0.251	–	−20.0
Sample A_3	−39.8	–	2.100	192.73	–	−48.7	–
Sample D_3	−37.5	–	0.184	186.57	–	−42.6	–
Sample F_3	−36.0	−10.0	0.475	228.01	0.304	−41.0	−20.0
Sample H_3	−37.0	−10.0	0.240	237.65	0.264	−40.0	−20.0
Sample J_3	–	−10.0	–	–	0.250	–	−29.1

two transitions corresponding to the NR and EVA phases, which indicates the incompatibility of the two components. As compared to the d.s.c. results, the dynamic mechanical analysis (d.m.a.) thermograms exhibit transitions at higher temperatures. This shows the difference in response of the molecular segments of the sample towards d.m.a. and d.s.c. analysis conditions. It can be seen that the tan δ_{max} due to the NR phase decreases as the EVA content increases, and the decrease is much sharper when the EVA content is 50% or more, where EVA forms a continuous phase.

As expected, the loss moduli (*Figure 7*) sharply increase in the transition zone until they attain maxima; they then decrease with increasing temperature. The T_g values obtained from the E'' *versus* temperature plots are always lower than those obtained from tan δ_{max} (*Table 4*). The sharp loss peaks indicate that the system components are incompatible. *Figure 8* shows the elastic modulus E' for various blends over a wide range of temperature. The curves for all the compositions have three distinct regions: a glass region, a transition region (leathery region), and a rubbery region. Since the experiment was not performed above 20°C, the high-temperature viscous region was not obtained. It is seen that the storage modulus decreases with increasing temperature due to the decrease in stiffness of the sample. The decrease is sharp in the case of high-NR blends.

The dynamic mechanical properties of crosslinked systems are shown in *Figures 9* to *17*. The important properties are listed in *Table 4*. It is seen that, as compared to the uncrosslinked blends, the T_g values of the NR phase increase sharply in the case of sulfur-crosslinked and mix-crosslinked systems. For example, the T_g of uncrosslinked, pure NR is −46.3°C. The corresponding values for sulfur-cured, peroxide-cured and mix-cured systems are −42.0, −46.0 and −39.8°C, respectively. Similarly, for the 70:30 NR:EVA blend the T_g values of the NR phase in the uncrosslinked, sulfur-cured, peroxide-cured and mix-cured systems are −46.3, −42.3, −46.0 and −37.5°C, respectively. This suggests that the degree of crosslinking of the NR phase is at a maximum in the case of the mixed crosslinking system. However, the T_g of EVA does not show a substantial shift with respect to crosslinking. This further suggests that in NR–EVA blends the extent of crosslinking of the NR phase is substantially higher than that of the EVA phase. This is associated with the faster curing nature of the NR phase as a result of the high level of unsaturation in the isoprene units.

In some recent studies on similar systems it was interpreted that the shift in T_g values is due to interface crosslinking which results in some type of compatibilization[20]. However, in the case of the NR–EVA system all the crosslinked systems show two transitions corresponding to the EVA and NR phases. Therefore, the crosslinked system components are incompatible. However, the observed shift in the T_g of the NR phase as seen from d.s.c. and d.m.t.a. studies may be associated with the predominant crosslinking of that phase and not due to the compatibilizing action.

The tan δ_{max} values of both the NR and EVA phases increase with crosslinking (*Figures 9*, *12* and *15*). The introduction of crosslinks also increases the storage moduli of the blends (*Figures 11*, *13* and *17*). The activation energy E of the transition of the NR phase has been calculated from the Arrhenius equation by plotting log(frequency) against the reciprocal of absolute temperature and finding out the slope of the straight line obtained. These data are given in *Table 4*. It can be noticed that in most cases, except for the mix-cured system, the activation energy decreases with increasing EVA content.

CONCLUSIONS

The thermal behaviour, morphology, crystallinity and dynamic mechanical properties of blends of natural rubber and ethylene–vinyl acetate have been investigated with special reference to the effect of blend ratio and crosslinking systems. The d.s.c. and d.m.t.a. results show that the blend components are incompatible in the crosslinked and uncrosslinked states. The predominant crosslinking of the natural rubber phase as a result of the addition of sulfur or mixed crosslinking agents can be analysed by the shift in the glass transition temperature of the natural rubber phase towards higher temperatures. The addition of natural rubber to EVA decreases the crystallinity of the samples, as endorsed by d.s.c. and X-ray analysis. The morphology of the blends, as studied by scanning electron microscopy, consists of a two-phase structure in which the natural rubber phase is dispersed into domains at its lower proportions. In 40:60 and 50:50 EVA:NR blends both phases exist as continuous phases. Phase inversion is observed when the proportion of EVA is less than 40%.

REFERENCES

1 Bruins, P. F. (Ed.) *Appl. Polym. Symp.* 1970, **15**
2 Platzer, N. A. J. (Ed.) *Adv. Chem. Ser.* 1971, **99**
3 Sperling, L. H. (Ed.) 'Recent Advances in Polymer Blends, Grafts and Blocks', Plenum Press, New York, 1974
4 Kempler, D. and Frisch, K. C. (Eds) 'Polymer Alloys: Blends, Blocks, Grafts and Interpenetrating Networks', Plenum Press, New York, 1977
5 Paul, D. R. and Newmann, S. (Eds) 'Polymer Blends', Vols I and II, Academic Press, New York, 1978
6 Roland, C. M. in 'Handbook of Elastomers' (Eds A. K. Bhowmick and H. L. Stephens), Marcel Dekker, New York, 1988, Ch. 6
7 Martuscelli, E., Riva, F., Sellitti, C. and Silvestre, C. *Polymer* 1985, **26**, 270
8 Martuscelli, E. *Polym. Eng. Sci.* 1984, **24**, 563
9 Locke, C. E. and Paul, D. R. *Polym. Eng. Sci.* 1973, **13**, 108
10 Kuriakose, B. and De, S. K. *Polym. Eng. Sci.* 1985, **25**(10), 630
11 Thomas, S., Gupta, B. R. and De, S. K. *J. Vinyl Technol.* 1987, **9**, 71
12 Koshy, A. T., Kuriakose, B. and Thomas, S. *Indian J. Nat. Rubber Res.* 1990, **3**(2), 87
13 Koshy, A. T., Kuriakose, B. and Thomas, S. *Polym. Degr. Stab.* 1992, **36**, 137
14 Koshy, A. T., Kuriakose B., Thomas, S. and Varghese, S. *J. Appl. Polym. Sci.* in press
16 Koshy, A. T., Kuriakose, B., Thomas, S. and Varghese, S. *Kausch Gummi Kunststoffe* 1992, **45**, 852
17 Gilby, G. W. (Ed.) 'Developments in Rubber Technology', Vol. III, Applied Science Publishers, London, 1982, pp. 101–144
18 Roychoudhury, N., Chaki, T. K., Dutta, A. and Bhowmick, A. K. *Polymer* 1989, **30**, 2047
19 Herman, P. H. and Weidinger, A. *Makromol. Chem.* 1961, **24**, 44
20 Tinker, A. J. *Rubber Chem. Technol.* 1990, **63**, 503